

DOI: 10.37943/14NEBW7927

Perizat Omarova

Master's degree, Postdoctoral, Department of Computer Science
omarova.peryzat2@gmail.com, orcid.org/0000-0001-9502-7959
Al-Farabi Kazakh National University, Kazakhstan

Timur Merembayev

PhD, Software Engineer
merembaevt@gmail.com, orcid.org/0000-0001-8185-235X
Institute Of Information And Computational Technology, Kazakhstan

Yedilkhan Amirgaliyev

Professor, Department of Computer Science
amir_ed@mail.ru, orcid.org/0000-0002-6528-0619
Institute of Information and Computational Technologies,
Al-Farabi Kazakh National University, Kazakhstan

MATHEMATICAL MODELING OF WATER MOVEMENT DURING A DAM BREAK USING THE VOF METHOD

Abstract. River valleys in mountainous areas are often subject to heavy rains and melting glaciers, resulting in the risk of mudflows and the destruction of hydraulic protective structures. In order to minimize the potential risk and negative outcomes of a disaster, both on an individual and environmental scale, it is crucial to possess essential information. This includes understanding the timing, location, and extent of flooding, as well as comprehending the force of water flow impact on protective structures. In the research, the numerical process of the movement of the water flow caused by the breakthrough of the dam is investigated. A two-dimensional numerical model of water flow during a dam break was constructed using the VOF method to describe the described process. With the help of the VOF method, the movement of the water surface is captured, while maintaining the law of conservation of mass. The mathematical model consists of Reynolds-averaged incompressible Navier-Stokes equations and includes the interphase equation. The turbulent k-e model was used to close the system of equations. The numerical algorithm used is PISO (Pressure-Implicit with Splitting of Operators). The obtained numerical results agree with the experimental data, indicating the developed algorithm's reliability and accuracy. The results are presented as comparative graphs and images showing the contour of the free surface movement along the experimental reservoir. A numerical model that has been tested in this way can provide significant support in preventing the devastating consequences of a dam break and providing timely assistance during the evacuation of the population.

Keywords: dam break, VOF method, PISO algorithm, numerical simulation

Introduction

Water is a vital resource for human civilization. An adequate and safe water supply is essential to our health, environment, society, and economy. Two major factors make this more important: coming climate change is making water supplies more irregular, drought trends are calling for more attention to water storage, and population growth is creating an increased demand for domestic, agricultural, and industrial water resources, with an emphasis on using irrigation for food production. Thus, the important role of dams throughout human history

will continue into the 21st century. Throughout the history of the world, dams have played an important role in storing and managing the water resources needed to sustain civilization.

At the same time, like any critical engineering structure, the construction of dams is a potential source of danger: the destruction of large dams can cause enormous damage to infrastructure, the environment and society and lead to a retreat in the development of the region. Thus, dam safety is an essential prerequisite for the sustainable development of reservoir projects or for the sustainable operation of existing ones. Indeed, dangerous technology has no future, and the history of dam construction spanning over 2,000 years shows that safety is the foundation of sustainable development. Maintaining the safety of dams requires the proper management of all safety elements, in particular, the maintenance of various structures, the restoration of identified deficiencies and aging components, the modernization and replacement of instruments where necessary, and the periodic review of the concept of emergency measures.

The causes of accidents accompanied by a breakthrough of hydraulic structures of the pressure front and flooding of coastal areas are most often:

1. Destruction of the foundation of the structure and insufficiency of spillways
2. The impact of the forces of nature (earthquake, hurricane, collapse, landslide)
3. Structural defects, violation of the rules of operation, and the impact of floods

Out of 300 dam accidents (accompanied by dam failure) in various countries over 175 years, in 35% of cases, the cause of the accident was the excess of the calculated maximum discharge flow (overflow of water over the crest of the dam).

There are several damaging factors in hydrodynamic accidents. In addition to the damaging factors characteristic of other floods (drowning, hypothermia), in case of accidents with hydrodynamically dangerous objects, the damage is caused mainly as a result of the action of a breakthrough wave. This wave is formed downstream due to the rapid fall of water from upstream.

The damaging effect of a breakthrough wave is manifested as a direct shock effect on people and the structure of a mass of water moving at high speed and the fragments of destroyed buildings, structures, and other objects moved by it. A breakthrough wave can destroy a large number of buildings and other structures. The degree of destruction will depend on their strength, as well as on the height and speed of the wave.

In case of catastrophic flooding, the threat to life and health of people, in addition to the impact of a breakthrough wave, is being in cold water, neuropsychic overstrain, and flooding (destruction) of systems that ensure the vital activity of the population.

Emergencies in the flood zone are often accompanied by secondary damaging factors, fires due to breaks and short circuits in electrical cables and wires, landslides and landslides as a result of soil erosion (Cao et al., 2004, [2]; Wu and Wang, 2008, [3]), infectious diseases due to contamination of drinking water and a sharp deterioration in the sanitary and epidemiological situation in settlements near the flood zone and areas of temporary accommodation of victims, especially in summer.

The consequences of accidents at hydrodynamically hazardous facilities can be difficult to predict. Being located, as a rule, within or upstream of large settlements and being objects of increased risk, if destroyed, they can lead to catastrophic flooding of vast territories, a significant number of cities and villages, economic facilities, mass deaths of people, a long cessation of navigation, agricultural and fisheries (Bahmanpouri et al., 2021, [1]).

Numerical modeling has been increasingly used to monitor the process of dam breakthroughs. Due to relatively low resource costs, numerical simulation based on computational fluid dynamics is very popular (Jeong et al., 2012, [4]; Simsek and Islek, 2023, [5]; Yang et al., 2022, [6]; Wang et al., 2020, [7]; Mukhamediev et al., 2023, [8]). To this end, the scientific

literature offers a huge range of numerical methods used to model the process of water flow propagation during a dam break. One of the applications of the computational fluid dynamics coupled with the discrete element method is the modeling of sand production in various media in research (Kazidenov et al., 2023 [9], Rakhimzhanova et al., 2022 [10]). This method allows you to model on micro-scale to solve the transport problem. In (Xu et al., 2023, [12]), a two-phase meshless method is used to reproduce the propagation of a breakthrough wave along various conditions of a wet bottom in the presence of bottom sediments. To show a more realistic simulation, the study's authors (Jafari et al., 2021, [13]) demonstrated the simultaneous change in the shape of the porous structure and the interaction of the breakthrough wave with it. For this, a combination of three numerical methods was used: FVM-VOF-DEM. In (Zhao et al., 2017, [14]), dam burst flows with different initial aspect ratios are modeled by the material point method (MPM) and shallow water equations (SWE). The material point method effectively models many materials and their relationships on a massive scale. Based on the SPH method, the study (Chang and Wu, 2023, [15]) evaluated the impact of different slopes in breakthrough wells on gentle and macro uneven slopes. Thus, numerical studies, although they allow some simplifications and consider idealized conditions, are improved by scientists every year, resulting in a real process of dam breakthrough close to natural conditions.

This study aims to create a dam burst flow simulation model and compares the experimental result with the numerical approach. The created model will be applied to the real Kazakhstan dams in further research.

VOF method

The VOF (Volume of Fluid Method) equation is a numerical method used to track the movement and deformation of interfaces between different phases in multicomponent flows. In this method, a variable is introduced, called the volume of liquid function (VOF), which represents the proportion of the volume of each phase in a given grid cell. The VOF equation defines the variation of this function in space and time, given the speed and movement of the interface between phases. The -VOF method is widely used in numerical models for modeling various physical phenomena, such as liquid flow through porous media, liquid spills, interaction of drops and bubbles, as well as mixing and phase separation processes. They provide more accurate and detailed modeling of interfaces between different phases and account for surface tension, making them useful tools in engineering and research.

The main idea of the liquid volume method is that for each computational cell there is one scalar value that fills these cells with one phase: water or air. For example, if some cell is empty, then the value is set to 0, and if vice versa, then the value is set to 1. Cells between 0 and 1 are in the interface and α represents the volume fraction of water, and $\alpha - 1$ the second fraction of the phase in the air cell. Thus, at the initial time $t = 0$ is distributed as $\alpha(x, y, z, t = 0)$, and then calculated as a solution to the transport equation:

$$\frac{\partial \alpha}{\partial t} + \frac{\partial(\alpha u_i)}{\partial x_i} = 0 \quad (1)$$

Since the position of the free boundary is determined by the equation $\alpha(x, y, z, t = 0)$, the physical properties of the gas-liquid mixture are found using the appropriate weighting coefficients [16]:

$$\rho = \alpha \rho_1 + (1 - \alpha)\rho_2, \quad \mu = \alpha \mu_1 + (1 - \alpha)\mu_2 \quad (2)$$

Indexes 1 and 2 mean two phases: air and water.

Mathematical model

To build a mathematical model, the laws of conservation of mass and momentum are used for an incompressible viscous isothermal fluid in the absence of mass and surface forces, as well as a system of Reynolds-averaged Navier-Stokes equations [16]:

$$\frac{\partial}{\partial x_i} (\rho u_i) = 0 \quad (3)$$

$$\frac{\partial}{\partial t} (\rho u_i) + \frac{\partial}{\partial x_j} (\rho u_i u_j + \rho \overline{u_i' u_j'}) = -\frac{\partial p}{\partial x_i} + \frac{\partial \tau_{ij}}{\partial x_j} \quad (4)$$

where u_i – is velocity components, p – is fluid pressure; μ – is dynamic viscosity, ρ – is liquid density, $\tau_{ij} = \mu \left(\frac{\partial u_i}{\partial x_j} + \frac{\partial u_j}{\partial x_i} \right)$ – is the mean tensor of viscous stresses. Averaging is performed over time and strokes mean the fluctuation part.

Turbulence kinetic energy k and velocity and ε rate of dissipation are determined from the transfer equation:

$$\frac{\partial(\rho k)}{\partial t} + \frac{\partial(\rho u_j k)}{\partial x_j} = \frac{\partial}{\partial x_j} \left[\left(\mu + \frac{\mu_t}{\sigma_k} \right) \frac{\partial k}{\partial x_j} \right] + P_k - \rho k \quad (5)$$

$$\frac{\partial(\rho \varepsilon)}{\partial t} + \frac{\partial(\rho u_j \varepsilon)}{\partial x_j} = C_{\varepsilon 1} \frac{\varepsilon}{k} P_k - \rho C_{\varepsilon 2} \frac{\varepsilon^2}{k} + \frac{\partial}{\partial x_j} \left(\frac{\mu_t}{\sigma_\varepsilon} \right) \frac{\partial \varepsilon}{\partial x_j} \quad (6)$$

where, $\mu_t = \rho C_\mu \frac{k^2}{\varepsilon}$ is turbulent viscosity, $P_k = \mu_t \left(\frac{\partial u_i}{\partial x_j} + \frac{\partial u_j}{\partial x_i} \right) \frac{\partial \overline{u_i}}{\partial x_j}$ is the rate of turbulence energy generation in the middle current. The coefficients of the model have the following standard values: $C_\mu = 0.09$, $C_{\varepsilon 1} = 1.44$, $C_{\varepsilon 2} = 1.92$, $\sigma_k = 1.0$, $\sigma_\varepsilon = 1.3$.

Numerical simulation algorithm

The numerical model for the test problem was presented using ANSYS, a widely used PISO (Pressure-Implicit with Splitting of Operators) numerical algorithm. PISO is one of the most common numerical simulation algorithms for solving the Navier-Stokes equations in non-stationary problems and software. In Ansys Fluent, the PISO algorithm is available as one of the numerical solver options when setting up a simulation. The PISO algorithm is used to solve non-stationary problems and is widely used in aerodynamics, hydrodynamics, and other areas where numerical simulation of flows and mass and momentum transfer is required. The steps of the PISO algorithm as a flowchart are presented in Figure 1.

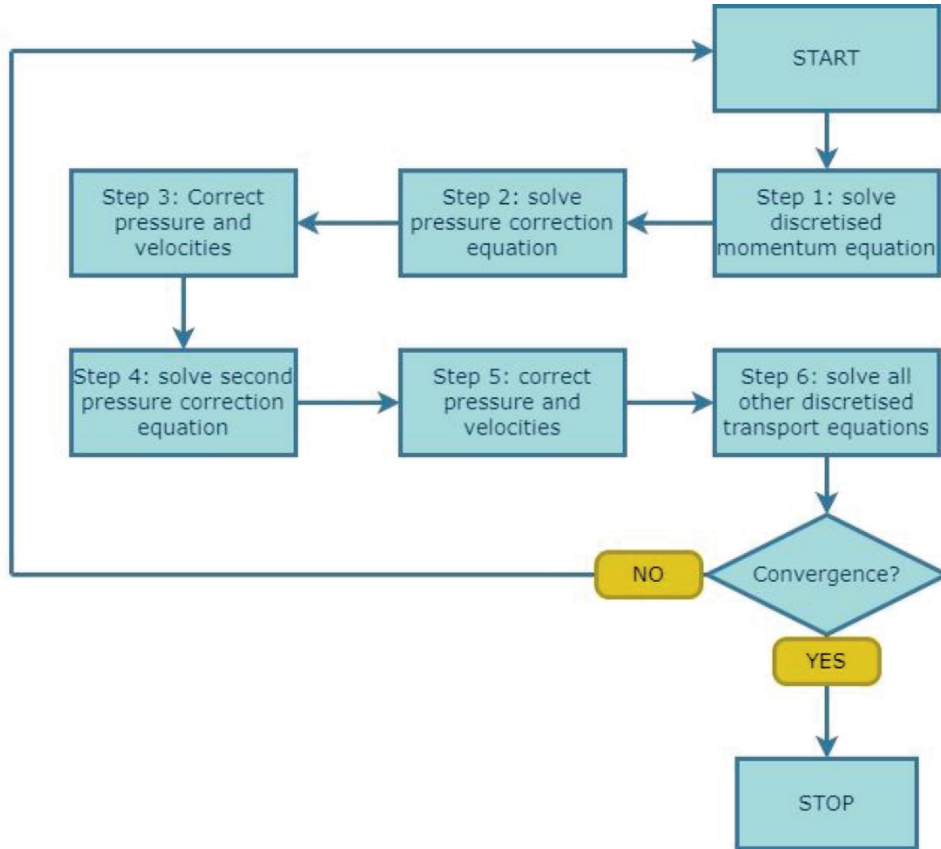


Figure 1. Flowchart PISO algorithm.

The PISO algorithm is a numerical method used to solve the Navier-Stokes equations for fluid flow. It stands for Pressure-Implicit with Splitting of Operators. The algorithm consists of two main steps: the predictor step and the corrector step.

The predictor step, we guess the pressure field p^* and obtain the velocity field components u^* and v^* using the discretized momentum equation. However, the initial assumption about the pressure may or may not be correct.

The corrector step 1, we determine correction coefficients for the pressure and velocity fields, as the velocity component obtained from the predictor step may not satisfy the continuity equation. We solve the momentum equation using the correct pressure field p^{**} to obtain the corresponding correct velocity components u^{**} and v^{**} .

$$\begin{aligned} p' &= p^{**} - p^* \\ u' &= u^{**} - u^* \\ v' &= v^{**} - v^* \end{aligned} \quad (7)$$

where, p^{**} , u^{**} , v^{**} correct pressure field and velocity component, p' , u' , v' – correction in pressure field and correction in velocity components, p^* , u^* , v^* guessed pressure field and velocity component. After correcting the pressure p' , we can find the correction components for the velocity u' , v' .

The corrector step 2, we add second corrections to the pressure and velocity fields to obtain the final, correct fields.

$$\begin{aligned} p^{***} &= p^{**} - p''; p'' = p^* - p' \\ u^{***} &= u^{**} - u''; u'' = u^* - u' \\ v^{***} &= v^{**} - v''; v'' = v^* - v' \end{aligned} \quad (8)$$

where, p^{***} , u^{***} , v^{***} correct pressure field and the correct velocity components, p'' , u'' , v'' – second correction pressure and velocity components, p^* , u^* , v^* – correct pressure and velocity components.

The PISO algorithm is widely used in computational fluid dynamics (CFD) simulations.

Numerical model validation

The test problem was solved numerically, based on an experimental study (Hu and Kashiwagi, (2004) [15]). Studies of the effect of flow on dam-break resistance are widely used as a test problem for various two-phase problems. This test problem was based on a dam-break flow experiment in a small reservoir. A 2D model was used to analyze the shock flow around the opposite wall and the pressure distribution over the given opposite wall. A schematic representation of the experimental reservoir is shown in Figure 2, where the length and height of the reservoir are $L_b=1.18\text{m}$, $L_h=0.3\text{m}$, respectively. A reservoir with water, height $H_{\text{water}}=0.12\text{m}$ and length $L_{\text{water}}=0.68\text{m}$, was opened when the vertical gate was suddenly removed. As shown in Figure 2, a pressure sensor was installed at point A to measure the pressure force of the water flow.

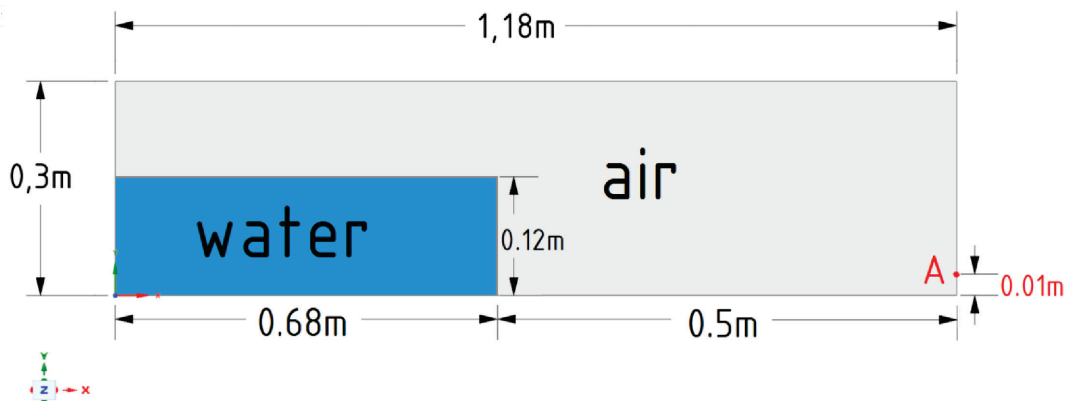


Figure 2. Test Problem Geometry

To perform the test task, an unstructured grid was built, the total number of elements of which was 29068, and the number of nodes was 14831. Figure 3 shows the computational grid of the study area. The total duration of the task calculation is 1200 seconds with a step of 0.001 seconds.

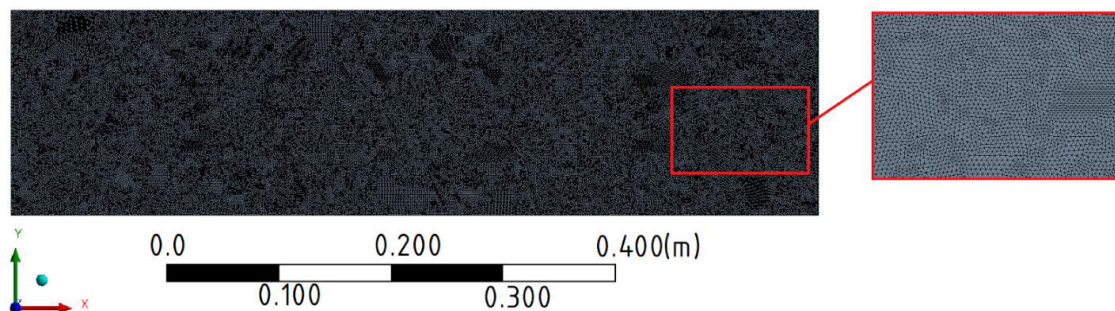


Figure 3. Computational grid for the test problem

The impact pressure results obtained were compared with the experimental and numerical values at point A. As can be seen from the results obtained, the first peak pressure occurs at the moment of impact, and the second peak pressure occurs when the overturning water hits the underlying water and causes the jet to splash. The obtained numerical simulation results are in good agreement with the experimental data (Hu and Kashiwagi, 2004, [15]). Figure 4 shows the results of the impact pressure on the opposite wall over time. The k-e RNG turbulent model was used for the test problem's numerical solution.

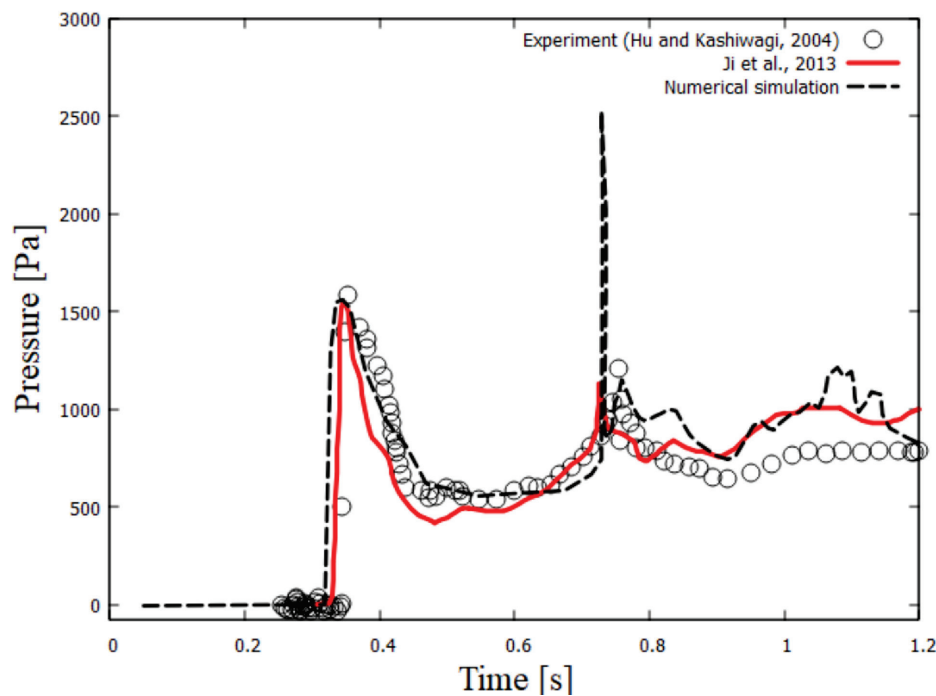
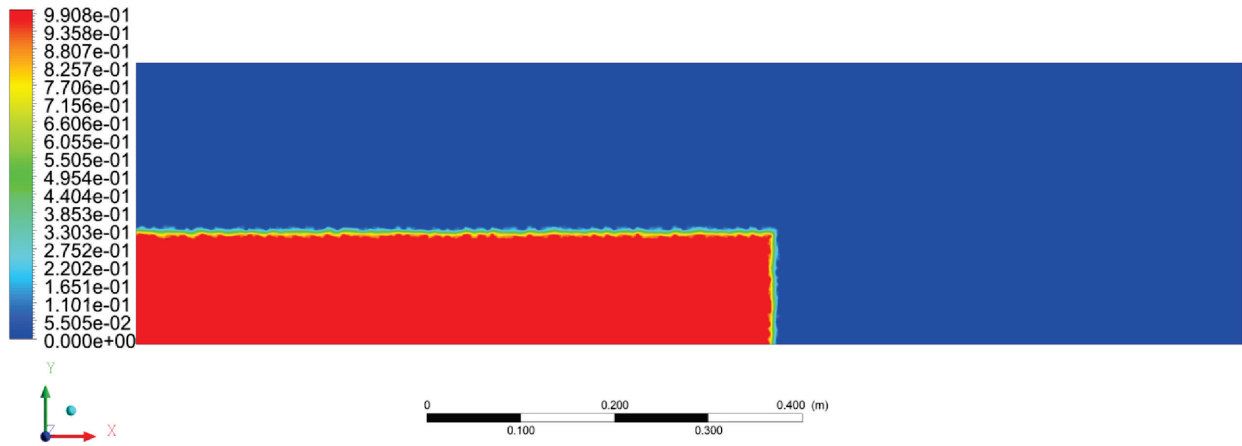


Figure 4. Water pressure for the flow during the dam break at different calculation times (0-1.2 sec).

The results show that when using the VOF method, many small droplets are formed close to the free surface. Moreover, at the initial moment, small drops in the flow are not noticed, and when the wave rises along the vertical wall and overturns back into the tank, only small drops and jets of water are noticeable.

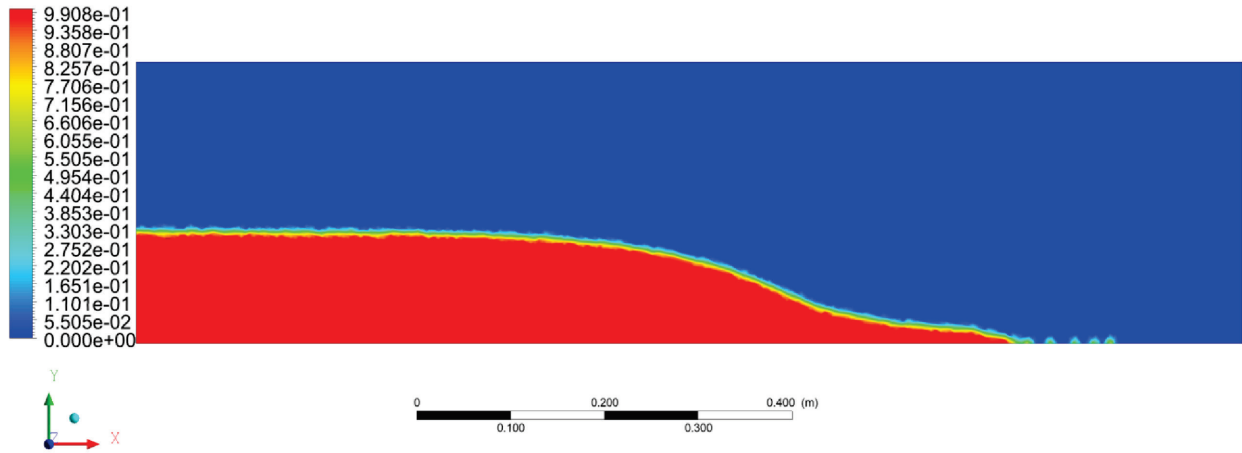
Figure 5 shows the contours of numerical calculations for various points in time. As can be seen, at $t=0$, at the moment of raising the vertical shutter, the water under the action of gravity moves to the right side, that is, where the reservoir is empty. This can be seen at $t=0.2$ sec, and at $t=0.4$ sec, the water reaches the right wall, hits under the force of inertia, and rises up. And already at $t=0.8$ sec, the force of gravity exceeds the force of inertia, and the water falls back into the tank and creates waves as a hook. As a result, reaching the extreme wall of the channel, the main flow forms the second wave at $t=1$ sec. At the last second, i.e. $t=1.2$ second, the inertia of the water decreases.

Water.Volume Fraction
Contour 1



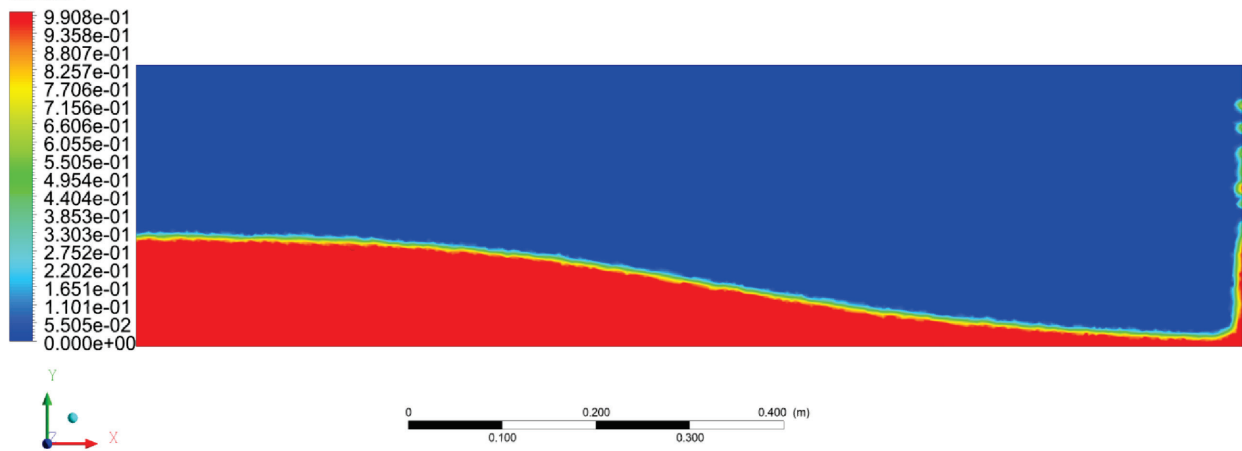
t=0 sec

Water.Volume Fraction
Contour 1



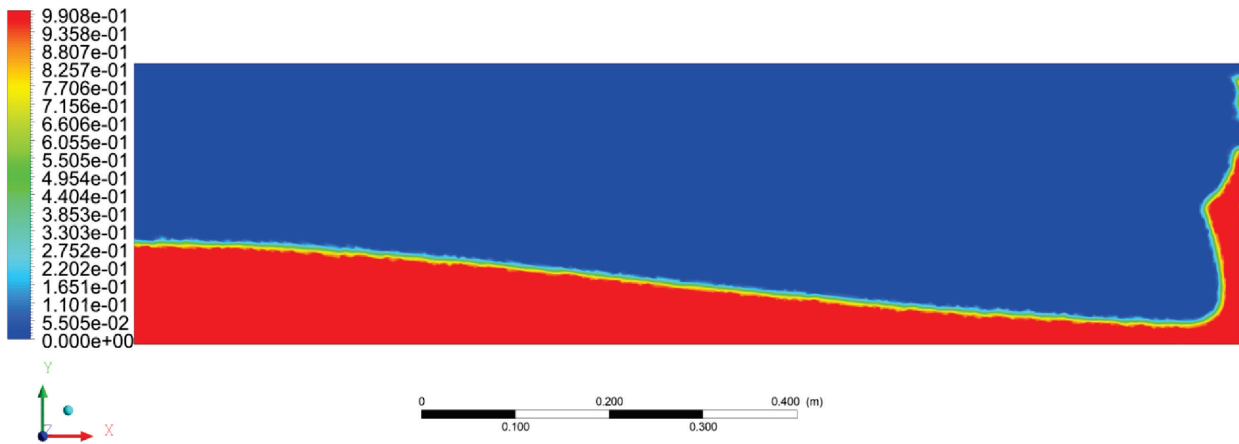
t=0.2 sec

Water.Volume Fraction
Contour 1



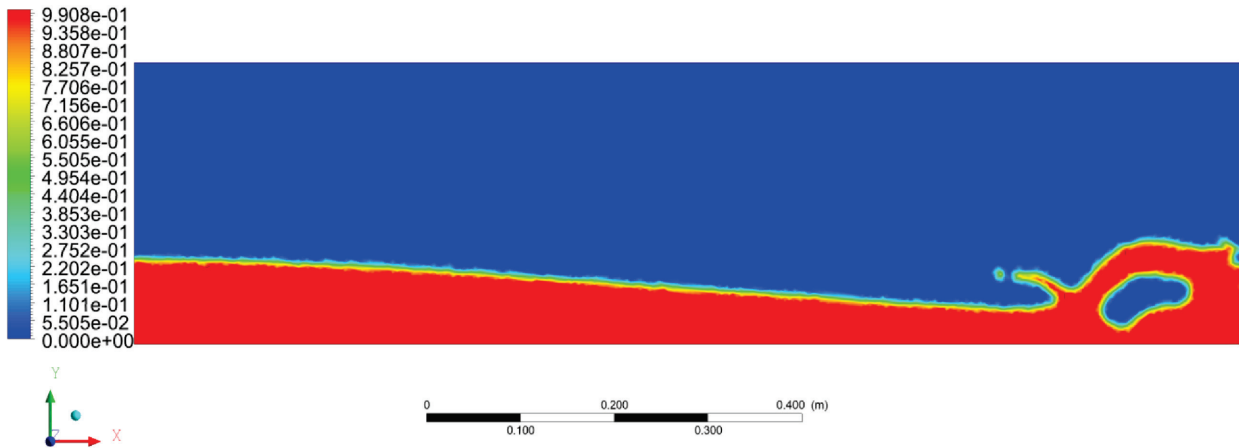
t=0.4 sec

Water.Volume Fraction
 Contour 1



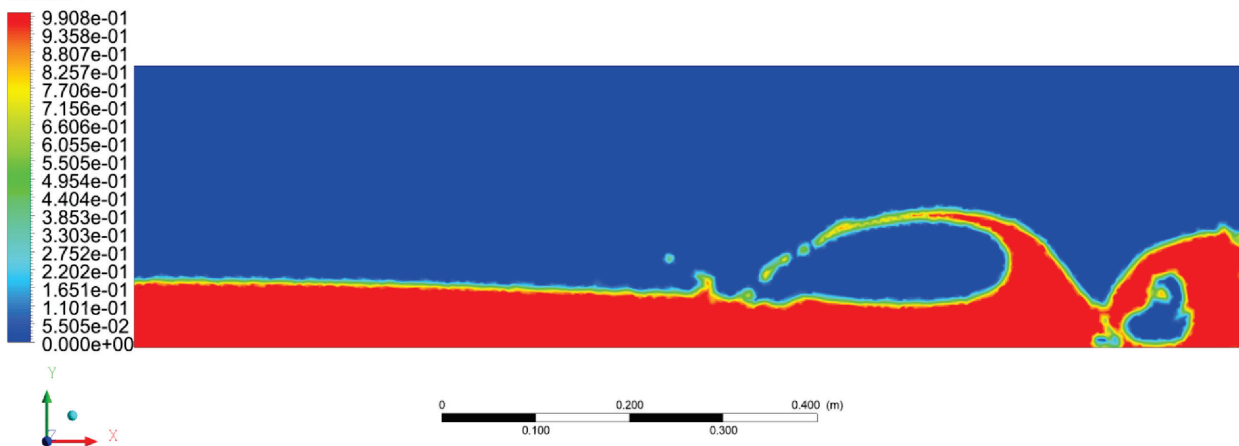
t=0.6 sec

Water.Volume Fraction
 Contour 1



t=0.8 sec

Water.Volume Fraction
 Contour 1



t=1 sec

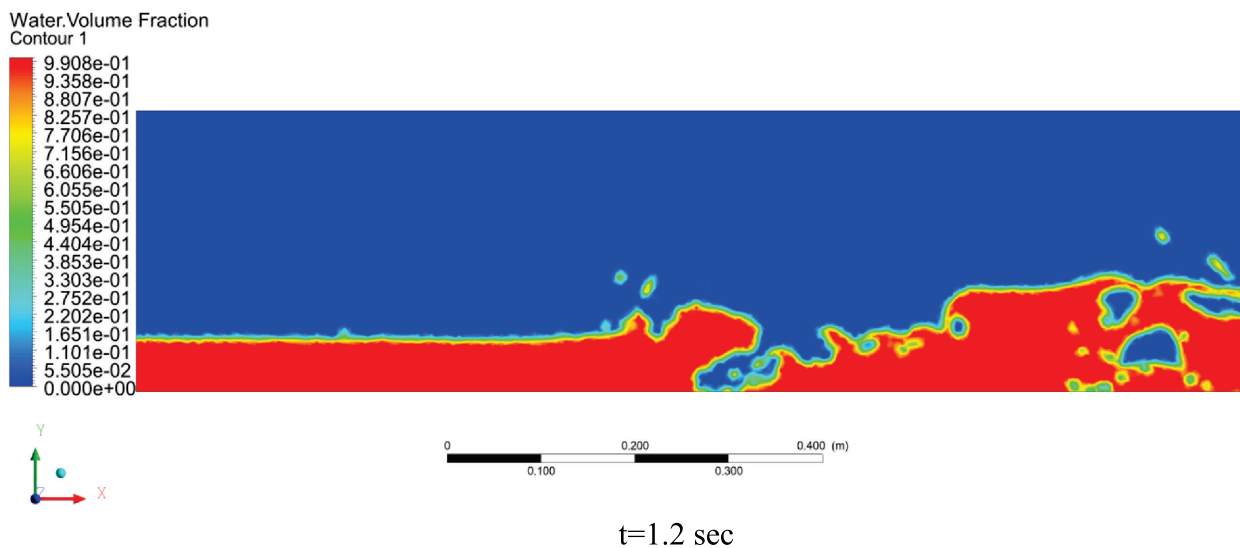


Figure 5. The contour of the change in water flow during a dam break at different times

Conclusion

This paper presents a numerical model using the VOF method for solving multiphase flow problems with complex free surface deformation. This model simulates dam burst flows and compares the experimental result with the numerical approach. For this task, the ratio of pressure and velocity was achieved using the PISO algorithm.

As a result, the obtained numerical results of modeling the dam breakthrough process based on the Navier-Stokes equations describing the dynamics of the interfacial mixture showed good agreement with experimental calculations. The results of this study can be used for real dams with difficult terrain to protect residents of nearby residential areas and the environment.

In the future, it is planned to improve the developed model by introducing other conditions in the form of a sedimentary layer, complex natural relief, obstacles in the way of the water flow, considering other numerical methods and their combinations, and much more.

Acknowledgement

The work was supported by grant funding from the Science Committee of the Ministry of Science and Higher Education of the Republic of Kazakhstan (BR18574144).

References

1. Bahmanpouri, F., Daliri, M., Khoshkonesh, A., Montazeri Namin, M., & Buccino, M. (2021). Bed compaction effect on dam break flow over erodible bed; experimental and numerical modeling. *Journal of Hydrology*, 594, 125645. <https://doi.org/10.1016/j.jhydrol.2020.125645>
2. Cao, Z., Pender, G., Wallis, S., & Carling, P. (2004). Computational Dam-Break Hydraulics over Erodible Sediment Bed. *Journal of Hydraulic Engineering*, 130(7), 689–703. [https://doi.org/10.1061/\(asce\)0733-9429\(2004\)130:7\(689\)](https://doi.org/10.1061/(asce)0733-9429(2004)130:7(689))
3. Wu, W., & Wang, S. S. Y. (2008). One-dimensional explicit finite-volume model for sediment transport. *Journal of Hydraulic Research*, 46(1), 87–98. <https://doi.org/10.1080/00221686.2008.9521846>
4. Jeong, W., Yoon, J.-S., & Cho, Y.-S. (2012). Numerical study on effects of building groups on dam-break flow in urban areas. *Journal of Hydro-Environment Research*, 6(2), 91–99. <https://doi.org/10.1016/j.jher.2012.01.001>

5. Simsek, O., Islek, H. (2023). 2D and 3D numerical simulations of dam-break flow problem with RANS, DES, and LES. *Ocean Engineering*, 276, 114298. <https://doi.org/10.1016/j.oceaneng.2023.114298>
6. Yang, S., Yang, W., Zhang, C., Qin, S., Wei, K., Zhang, J. (2022). Experimental and numerical study on the evolution of wave front profile of dam-break waves. *Ocean Engineering*, 247, 110681. <https://doi.org/10.1016/j.oceaneng.2022.110681>
7. Wang, B., Liu, W., Wang, W., Zhang, J., Chen, Y., Peng, Y., ... Yang, S. (2020). Experimental and numerical investigations of similarity for dam-break flows on wet bed. *Journal of Hydrology*, 124598. <https://doi.org/10.1016/j.jhydrol.2020.124598>
8. Mukhamediev, R., Amirgaliyev, Y., Kuchin, Y., Aubakirov, M., Terekhov, A., Merembayev, T., ... & Tabyrbayeva, L. (2023). Operational Mapping of Salinization Areas in Agricultural Fields Using Machine Learning Models Based on Low-Altitude Multispectral Images. *Drones*, 7(6), 357. <https://doi.org/10.3390/drones7060357>
9. Kazidenov, D., Khamitov, F., & Amanbek, Y. (2023). Coarse-graining of CFD-DEM for simulation of sand production in the modified cohesive contact model. *Gas Science and Engineering*, 113, 204976. <https://doi.org/10.1016/j.jgsce.2023.204976>
10. Rakhimzhanova, A., Thornton, C., Amanbek, Y., & Zhao, Y. (2022). Numerical simulations of sand production in oil wells using the CFD-DEM-IBM approach. *Journal of Petroleum Science and Engineering*, 208, 109529. <https://doi.org/10.31224/osf.io/pkteu>
11. Xu, T., Huai, W., Liu, H. (2023). MPS-based simulation of dam-break wave propagation over wet beds with a sediment layer. *Ocean Engineering*, 281, 115035. <https://doi.org/10.1016/j.oceaneng.2023.115035>
12. Jafari, E., Namin, M.M., & Badiiei, P. (2021). Numerical simulation of wave interaction with porous structures. *Applied Ocean Research*, 108, 102522. <https://doi.org/10.1016/j.apor.2020.102522>
13. Zhao, X., Liang, D., & Martinelli, M. (2017). Numerical Simulations of Dam-break Floods with MPM. *Procedia Engineering*, 175, 133–140. <https://doi.org/10.1016/j.proeng.2017.01.041>
14. Chang, C.-C., Wu, Y.-T. (2023). SPH modeling of dam-break bores on smooth and macro-roughness slopes. *Ocean Engineering*, 279, 114484. <https://doi.org/10.1016/j.oceaneng.2023.114484>
15. Hu, C., & Kashiwagi, M. (2004). A CIP-based method for numerical simulations of violent free-surface flows. *Journal of Marine Science and Technology*, 9(4), 143–157. <https://doi.org/10.1007/s00773-004-0180-z>
16. Ferziger J.H., & Peric M. (2002). *Computational Methods for Fluid Dynamics*. Springer-Verlag.